© 2016. Published by The Company of Biologists Ltd | Journal of Experimental Biology (2016) 219, 1110-1121 doi:10.1242/jeb.136168

RESEARCH ARTICLE

Adaptive plasticity of spino-extraocular motor coupling during locomotion in metamorphosing *Xenopus laevis*

Géraldine von Uckermann[1,*], François M. Lambert[1,*], Denis Combes[1,*,§], Hans Straka[2,‡] and John Simmers[1,‡]

ABSTRACT

During swimming in the amphibian *Xenopus laevis*, efference copies of rhythmic locomotor commands produced by the spinal central pattern generator (CPG) can drive extraocular motor output appropriate for producing image-stabilizing eye movements to offset the disruptive effects of self-motion. During metamorphosis, *X. laevis* remodels its locomotor strategy from larval tail-based undulatory movements to bilaterally synchronous hindlimb kicking in the adult. This change in propulsive mode results in head/body motion with entirely different dynamics, necessitating a concomitant switch in compensatory ocular movements from conjugate left–right rotations to non-conjugate convergence during the linear forward acceleration produced during each kick cycle. Here, using semi-intact or isolated brainstem/spinal cord preparations at intermediate metamorphic stages, we monitored bilateral eye motion along with extraocular, spinal axial and limb motor nerve activity during episodes of spontaneous fictive swimming. Our results show a progressive transition in spinal efference copy control of extraocular motor output that remains adapted to offsetting visual disturbances during the combinatorial expression of bimodal propulsion when functional larval and adult locomotor systems co-exist within the same animal. In stages at metamorphic climax, spino-extraocular motor coupling, which previously derived from axial locomotor circuitry alone, can originate from both axial and *de novo* hindlimb CPGs, although the latter's influence becomes progressively more dominant and eventually exclusive as metamorphosis terminates with tail resorption. Thus, adaptive interactions between locomotor and extraocular motor circuitry allows CPG-driven efference copy signaling to continuously match the changing spatio-temporal requirements for visual image stabilization throughout the transitional period when one propulsive mechanism emerges and replaces another.

KEY WORDS: Central pattern generator, Efference copy, Vestibulo-ocular reflex, Gaze control, *Xenopus* metamorphosis

INTRODUCTION

Retinal image stabilization during locomotion is crucial for all vertebrates in order to minimize the disruptive effects of self-generated movements on their ability to perceive the surrounding environment (Cullen, 2004, 2011, 2012). To maintain visual acuity, retinal image displacement is counteracted by dynamic compensatory eye and/or head adjustments that are traditionally attributed to the concerted actions of vestibulo-ocular and optokinetic reflexes (Angelaki and Cullen, 2008). However, recent evidence from both larval (Lambert et al., 2012) and young adult (von Uckermann et al., 2013) *Xenopus* frogs has indicated the involvement of an alternative mechanism whereby intrinsic copies of the rhythmic motor commands produced by spinal central pattern generator (CPG) circuitry are able to directly elicit eye movements appropriate for image stabilization, irrespective of locomotor mode. Thus, during undulatory tail-based swimming in pre-metamorphic tadpoles, such spinal efference copies produce alternating bursts in extraocular motor nerves supplying horizontal eye muscles to drive conjugate, left–right ocular movements (Combes et al., 2008; Lambert et al., 2012) that counteract rotational head movements in the horizontal plane (Azizi et al., 2007; Hoff and Wassersug, 1986).

By contrast, during post-metamorphic adult swimming produced by bilaterally synchronous hindlimb kicking, resultant head/body movements now consist of linear forward accelerations and decelerations during the powerstroke (extension) and returnstroke (flexion) phases, respectively, of each kick cycle (Combes et al., 2004; Beyeler et al., 2008). This in turn requires spino-extraocular motor coupling to generate bilaterally synchronous horizontal extraocular nerve activity for vergent eye motion (von Uckermann et al., 2013) to offset the disruptive visual effects of longitudinal translational forward motion (Rohregger and Dieringer, 2002). Therefore, the transmission of CPG efference copy signals to the extraocular motor nuclei not only provides an intrinsic predictive mechanism for driving gaze-stabilizing ocular adjustments during locomotion (Chagnaud et al., 2012), but also must undergo a developmental switch during metamorphosis to enable eye movement control to constantly correspond to the animal's change in body plan and mode of displacement.

The metamorphic transition of *Xenopus* from a fish-like larva to a quadrupedal adult is accompanied by the gradual emergence of limbs and regression of the tail along with the transformation of locomotory mode from tail-based (axial) to limb-based (appendicular) propulsion while the organism remains fully functional within its environment. Thus, at intermediate metamorphic stages, both larval and adult locomotor systems co-exist and can be employed conjointly or independently within the same animal at the transitional phase when one propulsive strategy is in the process of supplanting the other (Combes et al., 2004). This raises the question of how the interacting spinal locomotor and brainstem extraocular motor systems are able to continuously maintain effective gaze control in the face of the resultant change in visuo-motor demands.

To address this question, we used semi-intact or isolated *in vitro* preparations of *Xenopus laevis* (Daudin 1802) at critical metamorphic stages to record eye motion or extraocular motor nerve activity during spontaneous fictive swimming to explore the adaptive plasticity of spino-extraocular motor coupling (Straka and Simmers,

[1]Université de Bordeaux, Institut de Neurosciences Cognitives et Intégratives d'Aquitaine, CNRS UMR 5287, Bordeaux 33076, France. [2]Department Biology II, Ludwig-Maximilians-University Munich, Grosshaderner Str. 2, Planegg 82152, Germany.
*These authors contributed equally to this work
‡These authors contributed equally to this work

§Author for correspondence (denis.combes@u-bordeaux.fr)

Received 9 December 2015; Accepted 31 January 2016

Journal of Experimental Biology

Journal of Experimental Biology (2016) 219, 1110-1121 doi:10.1242/jeb.136168

2012). Our findings indicate that during metamorphosis, when the primary larval locomotor system is joined by a co-functional secondary adult system, efference copy signals for ocular movements can arise from the tail and hindlimb CPGs, either separately or in combination, with the latter's influence becoming increasingly dominant as metamorphosis proceeds.

MATERIALS AND METHODS

Animals

Experiments were performed on the South African clawed toad *Xenopus laevis* of either sex at developmental stages 55 (n=5), 59–62 (n=39) and 64–66 (n=5) (Nieuwkoop and Faber, 1956), either bred from an in-house laboratory colony or obtained from an authorized supplier and maintained at 20–22°C in aquaria exposed to a 12 h:12 h light:dark cycle. All experimental procedures were conducted in accordance with the European Communities Council Directive and the local ethics committee of the University of Bordeaux (#3301100012-A).

Semi-intact preparations

For *in vitro* experiments conducted on head-restrained, semi-isolated preparations (for video analysis of effective eye movements during fictive swimming) or completely isolated brainstem/spinal cord preparations (for electrophysiological recordings of spinal and extraocular motor output), animals were anesthetized in chilled frog Ringer's solution containing 0.05% 3-aminobenzoic acid ethyl ester (MS-222; Sigma-Aldrich, France). After opening of the skull and telencephalon removal, preparations were secured with insect pins in a Sylgard-lined Petri dish. To exclude any remaining body-/world motion-related sensory inputs, both optic nerves were transected and the bilateral vestibular endorgans were ablated. The spinal cord and ventral roots (VRs) were exposed until segments 20–25 and motor nerve branches innervating the hindlimb tibialis anterior (ankle flexor, Flex) and plantaris longus (ankle extensor, Ext) muscles, respectively (Beyeler et al., 2008) were identified according to their muscle targets and also dissected free. The rest of the tail and trunk was carefully removed and the isolated preparation (brainstem/spinal cord with the attached spinal motor nerves and extraocular motor innervation of the eyes) was transferred to a Sylgard-lined recording chamber after rinsing in fresh saline.

To monitor eye movements during fictive swimming in these preparations, the head was firmly secured dorsal-side up with insect pins to the Sylgard floor. For completely isolated brainstem/spinal preparations, which were also affixed dorsal-side up, the extraocular motor nerves innervating the medial rectus (MR) and lateral rectus (LR) muscles on both sides were disconnected from their respective muscle target to record impulse activity from the distal nerve stumps. In all experiments, preparations were continuously superfused with oxygenated (95% O_2, 5% CO_2) frog saline at a rate of 1.3–2.1 ml min^{-1} and maintained at 18±0.1°C with a Peltier cooling system.

Video analysis of eye movement

Video recording of binocular eye movements during fictive swimming was conducted on semi-isolated preparations using a high-speed digital camera (Grasshopper 03K2C, Point Grey Research) equipped with a micro-inspection zoom lens system (Optem Zoom 70XL, Qioptiq Photonics) operating at 100 frames s^{-1} (Lambert et al., 2012; von Uckermann et al., 2013). A coverslip was positioned above the head to reduce any mechanical disturbance of natural eye motion by circulating Ringer. Swimming-related movements of the eyes were video monitored along with simultaneous electrophysiological recordings of hindlimb and tail motor nerve activity (see below; Fig. 1A). Offline video analyses were conducted using free Fiji (National Institutes of Health) and OriginPro 8 (OriginLab Corporation) software. A region of interest was drawn around each eye and a binary threshold with respect to dark/light shading was used to produce a black/white ellipse-like image of the eye (Fig. 1B). The Fiji macro calculated frame-by-frame the angle between the major axis of the ellipse and an axis perpendicular to the body longitudinal axis. This fluctuating eye position angle was then plotted along with the associated electrophysiological signal(s).

Electrophysiology

Simultaneous extracellular recordings (A-M Systems model 1700 AC amplifiers) were made from LR and MR extraocular motor nerves, spinal VRs normally innervating tail (axial) muscles, and limb Flex and Ext motor nerves during episodes of spontaneous fictive swimming. Activity in limb Ext and Flex nerves was recorded with custom-made stainless steel wire electrodes isolated electrically with Vaseline (Combes et al., 2004). Extraocular motor nerves and spinal VRs were recorded unilaterally or bilaterally from cord segments 10–18 with manipulator-positioned, individually adjusted glass suction electrodes. Nerve activities were digitized at

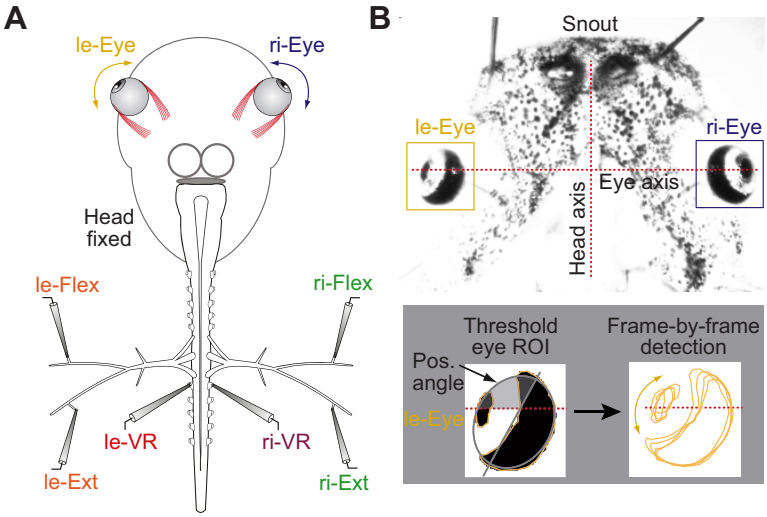

Fig. 1. Semi-intact preparations of metamorphosing *Xenopus laevis* used to monitor eye movements with fictive tail-based and limb-based locomotion. (A) Schematic of a semi-intact fixed head preparation (stage 60) used to record movements of the left (le) and right (ri) eyes along with discharge in bilateral spinal cord ventral roots (VRs) and hindlimb motor nerves (extensor, Ext; flexor, Flex) during episodes of fictive swimming. (B) Dorsal view of a head used to measure eye movements following frame-by-frame detection of eye position at a rate of 100 frames s^{-1} (lower panel) relative to the transverse axis through the two eyes (red dotted lines in upper and lower panels); eye position determination was facilitated by binary thresholding the outline of the eye within a region of interest (ROI).

Journal of Experimental Biology (2016) 219, 1110-1121 doi:10.1242/jeb.136168

10 kHz (CED 1401, Cambridge Electronic Design, UK), displayed and stored on computer for offline analysis with Spike2 software (Cambridge Electronic Design) using customized scripts.

Electrophysiological data analysis and statistics

Impulse discharge rates in individual extraocular and spinal motor nerves were measured by setting an amplitude threshold to count all impulses in a given multi-unit recording. Generally, firing rates (in spikes s^{-1}) were averaged (±s.e.) over 10–25 burst cycles for axial fictive swimming and 5–10 cycles for appendicular fictive swimming per preparation. The temporal relationship between simultaneously recorded spike discharges of selected nerve pairs during either mode of locomotor activity was determined using the cycle-to-cycle onset of each burst in a particular recording channel as the trigger for averaging the discharge rates of nerves recorded in other channels. A minimum of 10 axial and five appendicular burst cycles per preparation were used for this analysis.

In a complementary analysis, the phase-coupling between the respective activity of extraocular and spinal axial and/or limb motor nerves was evaluated using event correlations, with concurrent rhythmic bursting activity corresponding to a central peak in the cross-correlogram accompanied by regular satellite peaks on either side of the maximum (von Uckermann et al., 2013). All event cross correlations were preceded by autocorrelation analysis to verify the periodicity of burst activity expressed in individual extraocular, axial and hindlimb motor nerve recordings. Correlation coefficients indicating the strength of coupling between the respective discharges of nerve pairs during fictive axial- or limb-based locomotion and their probability levels (P-values) were calculated using the corrcoef function in MATLAB 7.1 (MathWorks). The extent of coupling between axial VR or limb Ext activity and associated LR/MR motor nerve activity was determined using the integrated traces of the extraocular nerve discharge as a function of the corresponding spinal motor activity during a given swim episode. Linear regression analyses by weighted least squares were made using Origin 6.1 software (Microcal). To then assess the change in strength of spino-extraocular motor coupling during the course of metamorphosis, the mean regression coefficients (r^2, ±s.d.) between ipsilateral MR and VR or Ext nerve activity during fictive swimming at four different developmental stages (n=7–8 swim episodes per stage group of 5 preparations, each episode comprising 6–24 burst cycles) were plotted. Differences between developmental stages in the coupling either between ipsilateral MR and VR (stages 55, 59/60 and 61/62) or between ipsilateral MR and Ext nerve activity (stages 59/60, 61/62 and 65) were evaluated using a nonparametric unpaired, one-way ANOVA (Kruskal–Wallis test; GraphPad Prism 4, GraphPad Software). Correlation coefficients (r^2) resulting from correlation or regression analyses and mean (±s.d.) values were taken to be significantly different at P<0.05.

RESULTS

The change in body plan and locomotor mode during *X. laevis* metamorphosis requires a concurrent switch in gaze-stabilizing strategy from conjugate left–right rotations of the tadpole's laterally positioned eyes to convergent eye movements in the post-metamorphic froglet (Rohregger and Dieringer, 2002) to maintain binocular visual field acuity (Finch and Collett, 1983). Here, to explore the dynamics of the developmental transition in underlying spino-extraocular motor control, we focused on specific intermediate stages of metamorphosis from the onset of climax (stage 59) until metamorphosis is largely completed at stage 62, over a period when both locomotor systems are present prior to secondary appendicular propulsion replacing the primary axial system with tail regression.

Bimodal fictive locomotion at metamorphic climax

In stage 59–61 *X. laevis*, the newly developed hindlimbs are fully functional, and a combination of bilaterally synchronous limb-kicking and left/right undulatory tail movements are used for body displacement (Fig. 2A) (Combes et al., 2004). Immediately after metamorphic climax at around stage 62, propulsive movements of the tail have declined and locomotion is now principally achieved by limb-kicking alone (Fig. 2B). After isolation *in vitro*, the

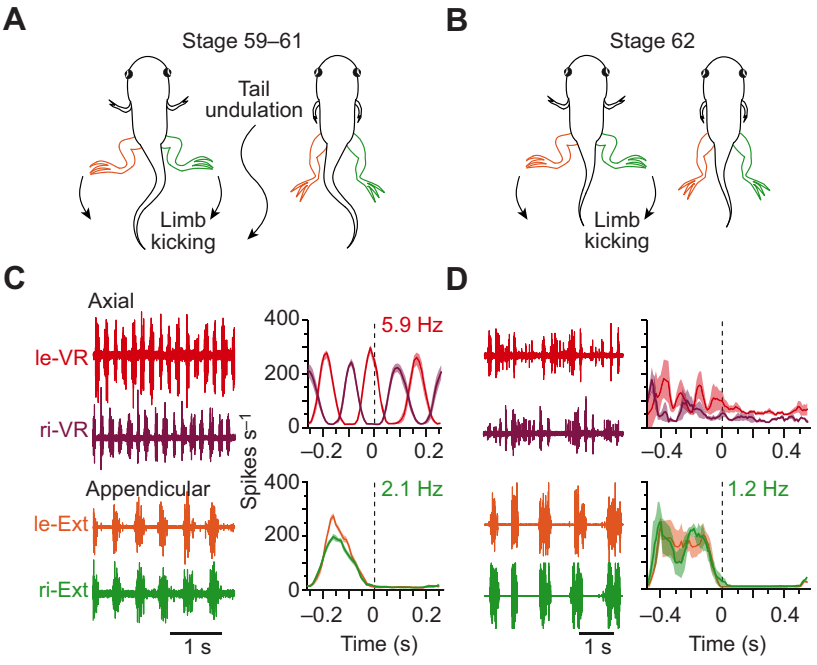

Fig. 2. Axial and appendicular locomotor rhythms at climax stages of *X. laevis* metamorphosis.
(A,B) Schematics depicting typical swimming movements that consist of combined undulatory tail- and limb-based propulsion at stage 59–61 (A), and exclusive bilaterally synchronous hindlimb kicking at stage 62 (B). (C,D) Typical episodes of spontaneous tail- and/or limb-based locomotor activity recorded in isolated brainstem/spinal cord preparations as temporally independent burst patterns in axial VRs and left/right hindlimb Ext motor nerves at stages 59/61 (C) and 62 (D). Plots at right in C,D show mean discharge rates (shaded areas are ±s.e.) in bilateral VRs and Ext nerves over a single locomotor cycle, averaged from 10 ri-Ext burst cycles (C) or from eight fictive limb-kick cycles (D). The vertical dashed lines (also in subsequent figures) indicate the mid-cycle of corresponding nerve discharge. Note the different cycle frequencies of axial and limb-kick rhythms at stage 59–61 and the strong extensor burst rhythm that is unrelated to the relatively weak axial VR discharge at stage 62.

Journal of Experimental Biology

Journal of Experimental Biology (2016) 219, 1110-1121 doi:10.1242/jeb.136168

brainstem/spinal cord of such animals during this transitional period continues to spontaneously generate the motor burst patterns that would normally drive axial or hindlimb muscle contractions underlying the two locomotor modes *in vivo* (Combes et al., 2004; Beyeler et al., 2008; Rauscent et al., 2009). As seen in the extracellular recordings of Fig. 2C (left panel), which were made in an isolated central nervous system (CNS) preparation from a stage 59–61 animal (see Fig. 2A), spontaneous bursting in axial VRs [left (le) and right (ri) VR], occurred independently of the slower rhythmic bursts recorded from the left and right hindlimb Ext motor nerves. Moreover, in correspondence with their behavioral expression *in vivo*, the separate fictive limb-kicking rhythm (here, mean cycle frequency 2.1 Hz) consisted of left/right extensor motoneurons firing in burst synchrony (Fig. 2C, lower right), whereas the faster axial rhythm (here, mean cycle frequency 5.9 Hz) consisted of bilateral VR motor bursting that alternated between the left and right sides of the cord (Fig. 2C, upper right). Similarly, in accordance with the predominance of appendicular propulsion in animals at post-climax (Fig. 2B), locomotor activity expressed spontaneously by isolated brainstem/spinal cord preparations at stage 62 (Fig. 2D, left panels) consisted of strong and regular extensor nerve bursting (here, mean cycle frequency 1.2 Hz), again occurring independently of the now diminished and disorganized axial VR motor activity (Fig. 2D, right plots; cf. upper right plots in Fig. 2C). These *in vitro* observations therefore indicated that during metamorphic climax, the coexisting spinal CPG networks that generate axial- and limb-based locomotor movements can spontaneously generate, either concurrently (as in Fig. 2C) or separately (see Fig. 3), coordinated patterns of burst activity that match the changing contributions of the two swimming behaviors *in vivo*.

Locomotion-related ocular movements at metamorphic climax

To determine whether functionally appropriate ocular movements driven by spinal CPG efference copies actually occur in these metamorphic hybrid animals, we used head-restrained, semi-isolated preparations (see Materials and methods) to monitor binocular eye motion simultaneously with the spike activity of axial spinal VRs and hindlimb extensor and flexor motor nerves during fictive swimming (Fig. 1). In such stationary head/isolated spinal cord preparations, in which the optic nerves had also been transected, locomotor-related eye movements continued to occur and thus were produced independently of any proprioceptive and optokinetic sensory feedback. Specifically, two distinct types of ocular motion were observed in association with the two different patterns of fictive locomotion: bilaterally alternating VR bursts (at 5–10 Hz; Fig. 3A) or slower (1–3 Hz) bilaterally synchronous

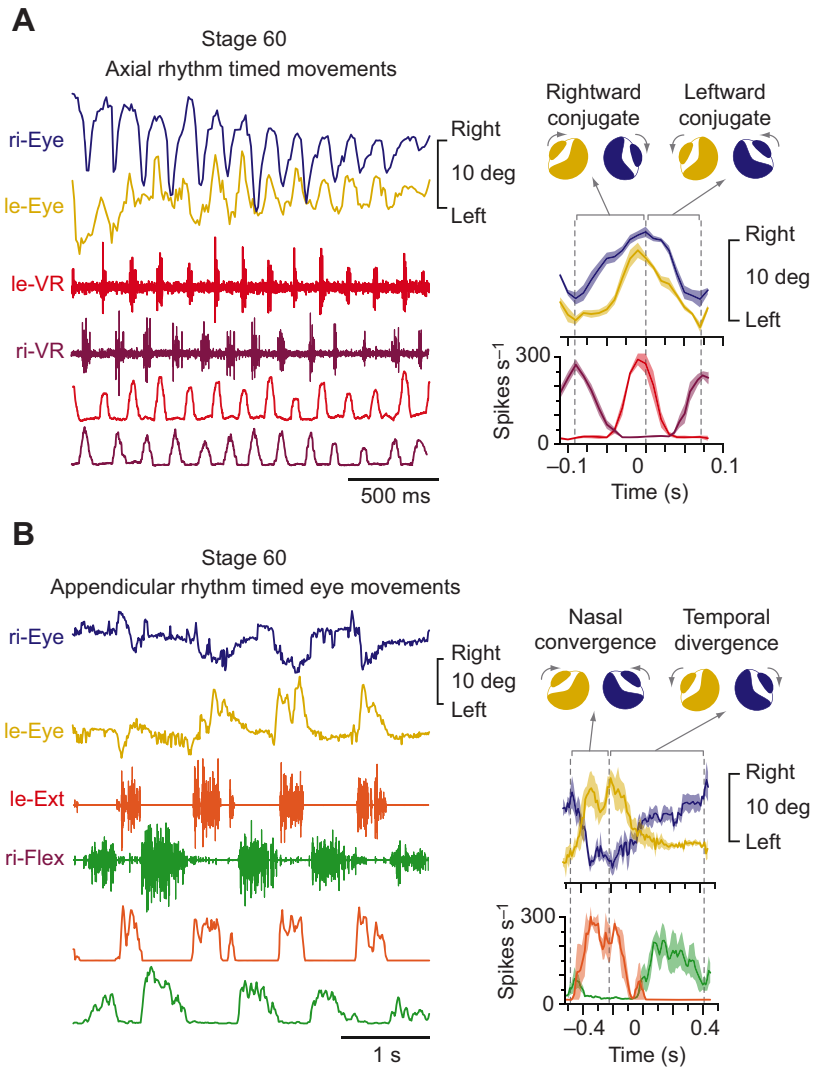

Fig. 3. Locomotor-related eye movements in pre-climax *X. laevis* during axial and appendicular fictive swimming. (A) Conjugate movements of both eyes in phase coordination with VR bursts during an episode of fictive axial swimming (left panel). Plots at right show mean (±s.e.) eye position angles (upper plots) and corresponding mean firing rates in VRs (lower plots) over a single locomotor cycle averaged from 10 burst cycles. Rightward eye movements were phase-coupled to bursts in the left VR and vice versa. (B) Convergent/divergent eye movements during a spontaneous episode of fictive appendicular swimming in the same preparation as in C. Plots at right show mean (±s.e.) modulation of bilateral eye position angles and corresponding mean firing rates in the left hindlimb Ext and right hindlimb Flex nerves over six consecutive cycles. Simultaneous nasal-directed movements of both eyes (ocular convergence) occurred in phase with Ext nerve bursts whereas divergent movements occurred conjointly with Flex nerve bursts.

Journal of Experimental Biology (2016) 219, 1110-1121 doi:10.1242/jeb.136168

extensor nerve bursts alternating with limb flexor bursts (Fig. 3B) that, respectively, underlie larval-like tail undulations and adult-like hindlimb kicking in the intact animal.

As seen during an episode of fictive axial swimming in an exemplary stage 60 preparation (Fig. 3A, left), both eyes exhibited rapid horizontal oscillations of ∼10 deg around a position slightly medial to each eye's initial resting position (upper two traces). Additionally, these ocular movements occurred in strict 1:1 coordination with the rhythmic burst discharge in simultaneously recorded left and right spinal ventral roots (le/ri-VR; Fig. 3A left, lower traces). Each le-VR burst was accompanied by a rightward rotation of both eyes (Fig. 3A, right) with an angular velocity that reached up to ±200 deg s^{-1}. Conversely, during the le-VR inter-burst interval, when the ri-VR became activated, both eyes performed a conjugate leftward rotation. Because the preparation was held immobilized with any head/eye motion detection experimentally suppressed, these ocular movements were occurring independently of visuo-vestibular sensory feedback signals that would normally arise during free undulatory swimming. Moreover, the oscillatory eye movements, which were being elicited by intrinsic efference copy signals from the spinal CPG itself, were appropriate for minimizing retinal image slip by counteracting actual body/head motion, in accordance with earlier findings in the pre-metamorphic tadpole (Lambert et al., 2012). Significantly, however, such larval undulatory swimming-related compensatory eye movements arising from the axial CPG alone were never observed in semi-isolated mid-metamorphic preparations beyond developmental stage 61.

In general, for animals older than stage 60, binocular horizontal eye movements were also observed during adult-like fictive appendicular swim episodes in semi-isolated preparations (Fig. 3B, left). In this case, bilateral ocular rotations occurred in a strict in-phase coordination with simultaneously-recorded hindlimb Ext nerve discharge (Fig. 3B, left), the latter corresponding to the forward propulsive phase of each swim kick cycle as in the post-metamorphic froglet (Combes et al., 2004; von Uckermann et al., 2013). In particular, the eye motion consisted of a convergent inward (nasal direction) rotation of both eyes (Fig. 3B, right) with an angular velocity up to ±200 deg s^{-1} in time with burst activity of the hindlimb Ext nerves on both sides. The convergent eye movements were then interrupted by alternating divergent, outward movements (temporal direction) to beyond their respective resting positions (Fig. 3B, right) during antagonistic Flex nerve bursts.

At metamorphic climax, when both axial- and limb-based propulsion are available, the two locomotor strategies can be separately expressed, as in the recordings shown in Fig. 3, which were from the same semi-isolated preparation, or, though even more rarely (∼20% of episodes), can occur in combination, as illustrated by the swim episode from a different stage 60/61 preparation in Fig. 4. Here, locomotor activity-related eye movements occurred only when ongoing axial VR bursts coincided with bilaterally synchronous limb Ext nerve bursts (Fig. 4A). The resultant ocular movement consisted of a mixture of rapid left–right conjugate eye movements coordinated with the VR bursts, which were superimposed on a slow alternating convergence of the two eyes during the course of each concurrent fictive limb extension (i.e. bilateral Ext nerve bursting; Fig. 4B).

There was also evidence for direct functional interactions between the spinal locomotor CPGs themselves (see also Combes et al., 2004; Rauscent et al., 2009), as indicated by the axial VR burst-timed modulation of both left and right Ext nerve burst discharge, and the reciprocal augmentation of axial burst amplitudes during each Ext burst (Fig. 4). In other semi-isolated preparations at or near metamorphic climax, concurrent leg Ext nerve and axial VR activity during fictive locomotion produced a general enhancement of ongoing eye rotations rather than separate convergent versus conjugate ocular movement (data not shown). Indeed, the occurrence of an Ext nerve burst could augment an ocular displacement elicited during a conjoint axial VR discharge by up to 20 deg. However, it remains unknown whether this facilitation of ongoing eye movement when axial and Ext bursts coincide (also see below) is due to separate ascending influences from the two spinal CPGs, or arises indirectly via one active CPG network exerting a global excitatory influence on the other within the spinal cord. Nonetheless, together, these findings indicate that the expression of larval- and/or adult-like locomotor programs at metamorphic climax stages can indeed elicit eye motion patterns originating from either the axial or appendicular CPG networks, or both, presumably to

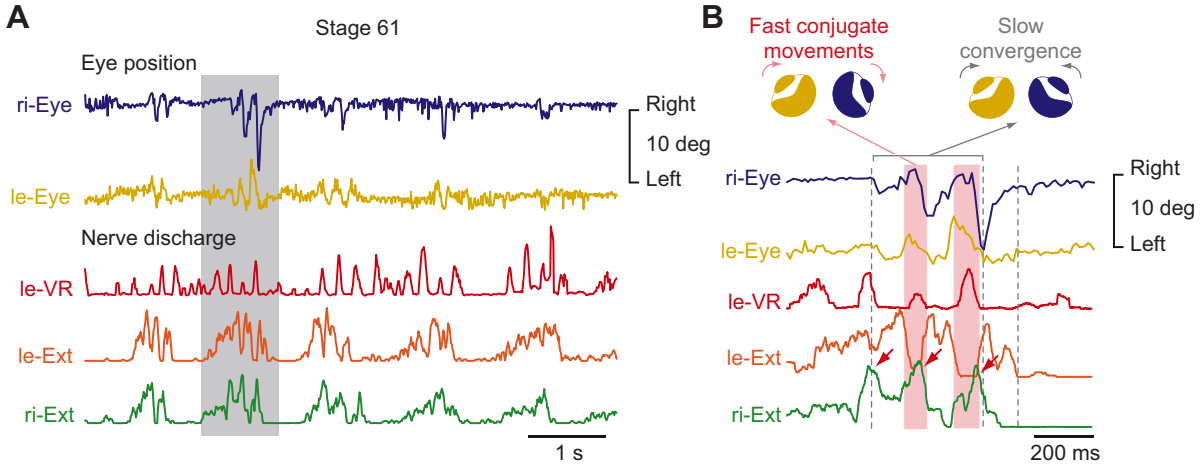

Fig. 4. Eye movements during coincident axial and appendicular fictive swimming at metamorphic climax. (A) Binocular eye movements during an episode of combined axial and appendicular fictive swimming in a semi-intact stage 61 preparation. Note that eye movements occurred solely during bilaterally synchronous hindlimb Ext bursts. (B) Higher magnification of a single Ext burst (gray shaded area in A), illustrating the mixture of rapid, axial-timed conjugate eye movements (light red shaded area) superimposed on slow Ext burst-timed convergent displacements. Also note axial burst-timed influences on bilateral Ext nerve activity (red arrows in B).

Journal of Experimental Biology

Journal of Experimental Biology (2016) 219, 1110-1121 doi:10.1242/jeb.136168

satisfy visual image-stabilizing demands during head/body motion resulting from the combinatorial expression of the two propulsive behaviors.

Spino-extraocular motor coupling prior to metamorphic climax

To further examine the respective contributions of intrinsic axial and appendicular CPG signaling to extraocular motor control, we recorded from the abducens and oculomotor motor nerves that normally innervate the horizontal LR and MR eye muscles, respectively, along with spinal VRs and hindlimb motor nerves in the completely isolated CNS of animals approaching metamorphic climax (stage 59/60; Fig. 5). Such *in vitro* preparations continued to co-express the two distinct rhythmic burst patterns (Fig. 5Ai,Bi) that corresponded to larval-like tail-based undulatory swimming and bilaterally synchronous hindlimb kicking as in the adult froglet (see Fig. 2) (Combes et al., 2004). Moreover, during such spontaneous episodes of locomotor activity at stage 59/60, LR and MR extraocular motor nerves displayed rhythmic, bilaterally alternating bursting (Fig. 5Aii,Bii, upper plots) that was in close coordination with axial VR discharge (Fig. 5Aii,Bii, lower plots), as confirmed by correlation analysis that showed highly regular burst recurrences at the same VR-timed cycle frequency (Fig. 5Aiv,Biv, upper red correlograms). In correspondence with the production of gaze-stabilizing eye movements during real behavior, burst discharge in the synergistic right LR (blue plot in Fig. 5Aii) and left MR nerves (yellow plot in Fig. 5Bii) occurred in-phase with axial bursts on the left side of the cord, whereas bursts in the left LR and right MR were in phase with VR bursts on the opposite cord side (yellow and blue plots in Fig. 5Aii and Bii, respectively). Thus the temporal relationship between axial VR and LR/MR nerve activity at a developmental stage immediately prior to metamorphic climax was equivalent to that of younger pre-metamorphic larvae where conjugate left–right ocular movements occur in phase-opposition to tail/head oscillations during swimming (Lambert et al., 2012).

In contrast, only a weak interaction was observed between LR (Fig. 5Ai,Aiii) and MR (Fig. 5Bi,Biii) nerve activity and the accompanying slower appendicular rhythm, which exerted little influence on the cycle-to-cycle timing of discharge in the two extraocular motor pools (Fig. 5Aiv,Biv, lower green correlograms). However, in both cases, a significant enhancement in amplitude of ongoing axial-timed extraocular nerve discharge was typically apparent during hindlimb extensor burst activity. In the experiment illustrated in Fig. 5A, although left and right LR bursts remained strictly coordinated with the axial rhythm, their amplitudes were significantly increased by ∼60% [57.7±9.0% (s.e.); Mann–Whitney *U*-test, $U=3$, $P=0.015$] during each Ext burst (Fig. 5Aiii). Similarly, the amplitude of bilateral, axial-coupled MR nerve discharge in the experiment shown in Fig. 5B was increased by more than 100% (126.4±10.0%; Mann–Whitney *U*-test, $U=0$, $P=0.002$) during each Ext nerve burst (Fig. 5Biii). Together, these *in vitro* data, which

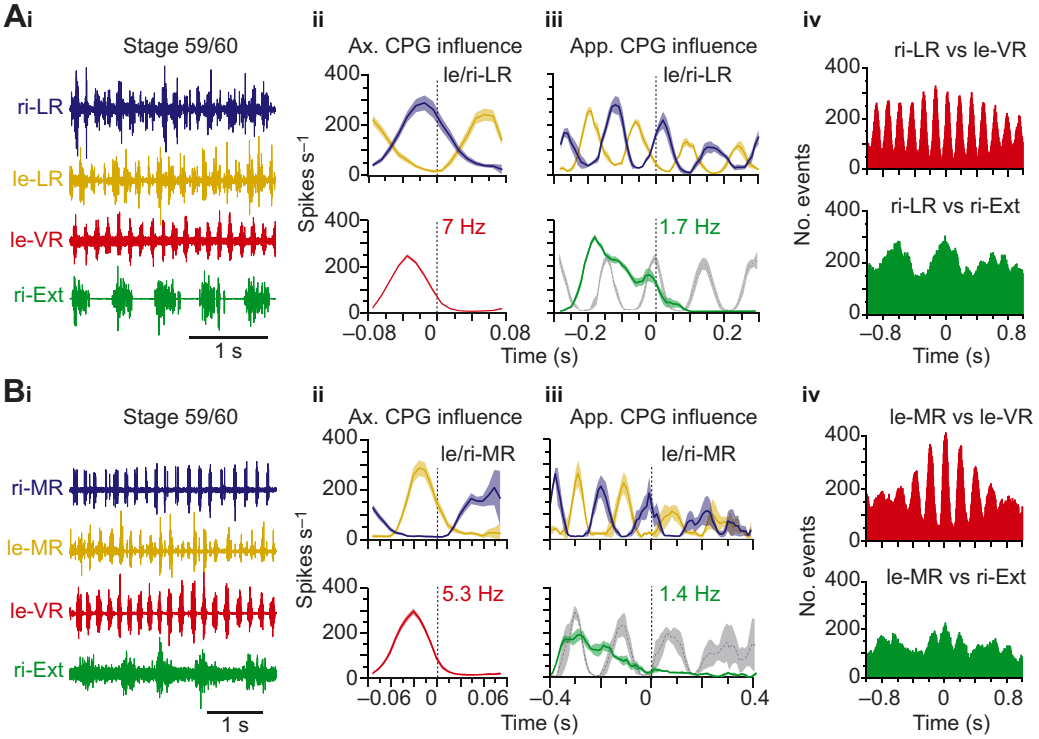

Fig. 5. Spino-extraocular motor coupling during spontaneous bimodal fictive swimming at pre-climax. (A,B) During episodes of co-expressed fictive tail- and limb-based swimming in two different isolated stage 59/60 preparations, burst discharge in left and right lateral rectus (LR; A) and medial rectus (MR) nerves (B) occurred in time with the faster axial VR burst rhythm (Ai,Bi). Mean (±s.e.) firing rate modulation over a single axial rhythm cycle (LR, Aii; MR, Bii; averaged from 23 and 21 consecutive le-VR bursts, respectively), and an appendicular rhythm cycle (LR, Aiii, MR, Biii; averaged from eight and six ri-Ext bursts, respectively). (Aiii,Biii) Concomitant mean le-VR firing rates (grey traces) during the corresponding slower Ext burst cycle; MR and LR bursts were in phase with axial VR rhythmic discharge on ipsi- and contralateral sides, respectively. Note the amplitude enhancement of axial-timed LR and MR discharge during Ext bursts (black arrows). (Aiv,Biv) Cross-correlograms showing strong in-phase coupling between ri-LR and contralateral le-VR bursts (upper red plot in Aiv; $r^2=0.88$, $P<0.001$) and between le-MR and ipsilateral le-VR bursts (upper red plot in Biv; $r^2=0.69$, $P<0.001$). Note the detectable, yet statistically insignificant modulation of LR and MR activity in time with Ext bursts (lower green plots in Aiv, $r^2=0.02$, $P=0.012$, and Biv, $r^2=0.02$, $P=0.05$).

Journal of Experimental Biology (2016) 219, 1110-1121 doi:10.1242/jeb.136168

concur with previous findings from eye motion recordings, indicate that at early metamorphic climax, spino-extraocular motor coupling remains closely associated with tail- rather than limb-based locomotion, although an influence from the *de novo* appendicular CPG, possibly by local intraspinal influences, on the strength (but not the frequency) of axial rhythmogenesis itself is beginning to emerge.

Transitional changes in spino-extraocular motor coupling at metamorphic climax

In contrast to the situation at pre-climax, where spino-extraocular motor influence arises almost exclusively from the axial CPG network, closer to or at metamorphic climax (stages 60/61), fictive swimming-related extraocular motor responses elicited by the hindlimb CPGs were found to become increasingly preponderant. The gradual increase in the lumbar CPG's control of the extraocular motor system in parallel with a progressive loss of axial CPG influence during this crucial climax period could be seen in swim episodes expressed spontaneously by different *in vitro* preparations in which the co-functional axial and hindlimb CPGs were found to exert variable influences on extraocular motor output. In this context, it is relevant to bear in mind inter-individual differences in the precise timing over which this functional transition occurs. A given experimental preparation previously identified on morphological grounds as originating from a stage 60/61 animal, for example, could express functional spino-extraocular coupling relationships that occur developmentally earlier or later compared with those found in other apparently similarly aged animals. Despite this variability, however, a number of consistent developmental steps could be recognized.

An initial indication of the shift in predominance of axial versus appendicular CPG–extraocular coupling was discernible when rhythmic lumbar CPG burst activity, independently of the separate faster axial CPG rhythm, had begun to influence the actual timing of extraocular motor discharge. This secondary spino-extraocular influence is evident in the representative example shown in Fig. 6, where the left MR and the contralateral right LR nerves, whose co-activation underlies conjugate eye movement in the pre-metamorphic tadpole, were monitored during fictive bimodal axial and appendicular swimming in a stage 60/61 *in vitro* preparation (Fig. 6A). As expected, the two extraocular motor populations increased their firing rates during each spinal le-VR burst (Fig. 6B), but separate bursts in both nerves were also co-expressed in time with the accompanying hindlimb extensor rhythm (Fig. 6C). This simultaneous in-phase relationship with the two locomotor rhythms was confirmed by cross-correlation analysis of the coupling between the MR nerve activity and both appendicular Ext and axial VR discharge (Fig. 6D).

Furthermore, the timing of the developmental switch to an adult spino-extraocular coupling relationship could progress differently in the two horizontal extraocular motoneuronal pools, as indicated by another stage 60/61 preparation (Fig. 7). Here, during spontaneous fictive tail- and limb-based swimming (Fig. 7A), axial CPG coupling with MR motoneurons had virtually disappeared (Fig. 7B, upper plot; 7D, lower red correlogram) and was replaced by a strong appendicular CPG drive (Fig. 7C, upper plot; 7D, upper green correlogram). Conversely, bursts that were still alternating in left–right LR nerves also remained strictly time-locked to axial CPG activity (Fig. 7B, middle plots; 7D, upper red correlogram), whereas a significant influence of the appendicular CPG on the two LR motor pools had still not emerged (Fig. 7C, middle plots; 7D, lower green correlogram).

The approaching completion of the transition to exclusive lumbar CPG-derived spino-extraocular coupling was generally evident at early post-climax stages, where strong, extensor-timed bursts were expressed in both the LR and MR motor nerves, with little or no remaining discernible contributions from the axial CPG, whose own activity had already begun to weaken and become more irregular. This penultimate step is illustrated by the stage 61/62 preparation in Fig. 8, where during combined fictive axial and appendicular swimming (Fig. 8A), a robust hindlimb Ext burst-timed discharge (Fig. 8C, lower plot) occurred in bilateral MR nerves (Fig. 8C, upper plots; 8D, upper green correlograms). In contrast, although axial CPG-timed modulation of left and right MR nerve activity persisted (Fig. 8B, upper and lower plots; 8D, lower red correlograms), this influence now tended to produce synchronous activation of these two bilateral nerves (see arrow in upper Fig. 8B) rather than larval-like burst alternation. Furthermore, a significant axial CPG-timed influence on LR motoneurons no longer occurred (Fig. 8B, middle plot). This coupling pattern, which involved a further enhancement of bilaterally synchronous lumbar CPG drive to MR motoneurons in particular, thus increasingly resembled the spino-extraocular influence that is ultimately responsible for convergent eye

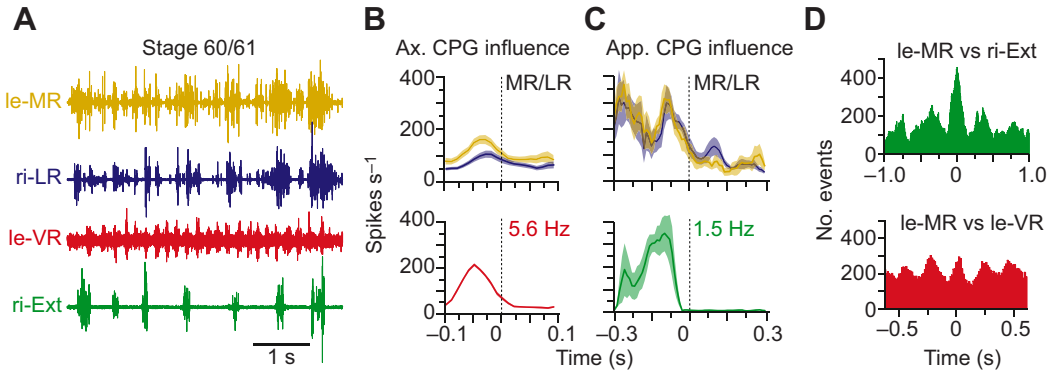

Fig. 6. Spino-extraocular motor coupling during spontaneous bimodal fictive swimming at metamorphic climax. (A) Burst discharge in synergistic left MR and right LR nerves in an isolated stage 60/61 preparation during an episode of co-expressed fictive tail- and limb-based swimming. (B,C) Mean (±s.e.) MR and LR firing rate modulation over a single axial rhythm cycle (B; averaged from 18 consecutive le-VR bursts) and appendicular rhythm cycle (C; averaged from seven ri-Ext bursts). Note that le-MR and ri-LR nerve activities (upper plots) were strongly phase-coupled to both the axial VR as well as the Ext burst rhythm. (D) Cross-correlograms confirming the in-phase relationship between le-MR and ri-Ext rhythmic bursting (upper green plot, r^2=0.56, P<0.05), and a persistent significant influence of the axial rhythm (lower red plot; r^2=0.43, P<0.05) on MR nerve activity.

Journal of Experimental Biology

Journal of Experimental Biology (2016) 219, 1110-1121 doi:10.1242/jeb.136168

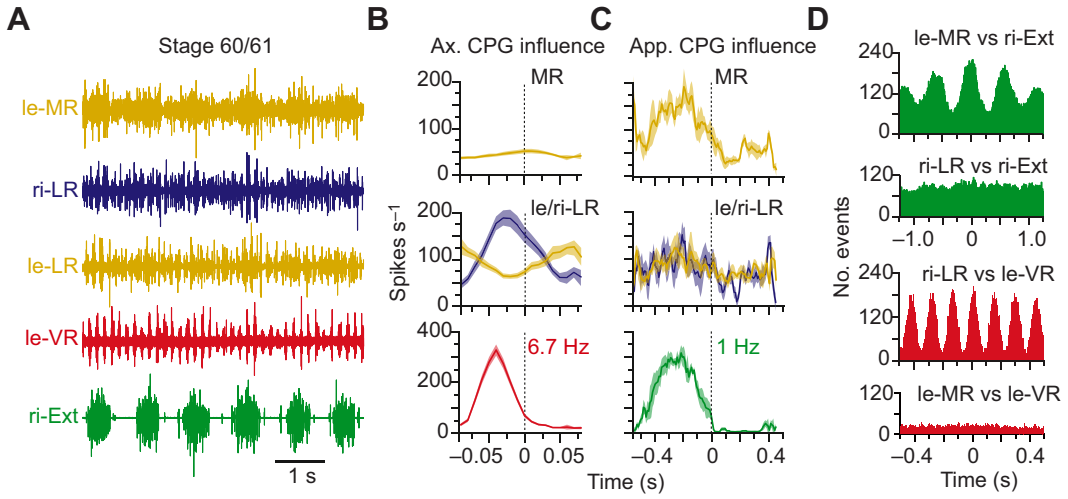

Fig. 7. Differential influence of co-expressed axial and appendicular locomotor rhythms at metamorphic climax. (A) Burst discharge in MR and bilateral LR nerves during an episode of combined axial- and limb-based fictive swimming in an isolated stage 60/61 preparation. (B) Mean (±s.e.) MR and LR firing rate modulation over a single axial rhythm cycle (averaged from 24 consecutive le-VR bursts) illustrating a strong phase-coupling of le-LR/ri-LR bursts (yellow and blue traces, respectively, in middle plot) but a weak coupling of le-MR bursts (yellow trace in upper plot) with the axial le-VR rhythm (red trace in lower plot). (C) Mean (±s.e.) firing rate modulation over a single appendicular burst cycle (averaged from six ri-Ext burst cycles). Note that bilateral LR activity was weakly influenced by the appendicular Ext burst rhythm, in contrast to le-MR nerve discharge (yellow trace in upper plot), which was strongly modulated in phase with ri-Ext bursts. (D) Cross-correlograms confirming the strong in-phase coupling of ri-LR and axial (le-VR) bursting (upper red plot, r^2=0.71, P<0.001) but an absence of coupling with ri-Ext bursts (lower green correlogram; r^2=0.004, P=0.39). In contrast, le-MR nerve discharge was unrelated to axial VR bursting (lower red correlogram; r^2=0.002, P=0.57), but strongly phase-coupled to the Ext appendicular rhythm (upper green correlogram; r^2=0.66, P<0.001).

movements during solitary limb-kick propulsion in the post-metamorphic froglet after tail resorption (von Uckermann et al., 2013).

In a final analysis, the dynamics of the interchange in axial and hindlimb locomotor CPG control of extraocular motor activity during *X. laevis* metamorphosis was assessed by a linear regression analysis of MR nerve discharge as a function of simultaneously recorded spinal VR or hindlimb motor nerve activity during episodes of fictive swimming (see Materials and methods). Mean correlation coefficients for the linear regression, which in turn indicated the strength of coupling between spinal CPG and corresponding MR activity, were compared at different developmental stages (Fig. 9A). In accordance with the respective exclusive CPG influence on the extraocular motor system, relatively high coefficients were observed in the tadpole (stage 55) and froglet (stage 65), at times when axial- and limb-based locomotor strategies

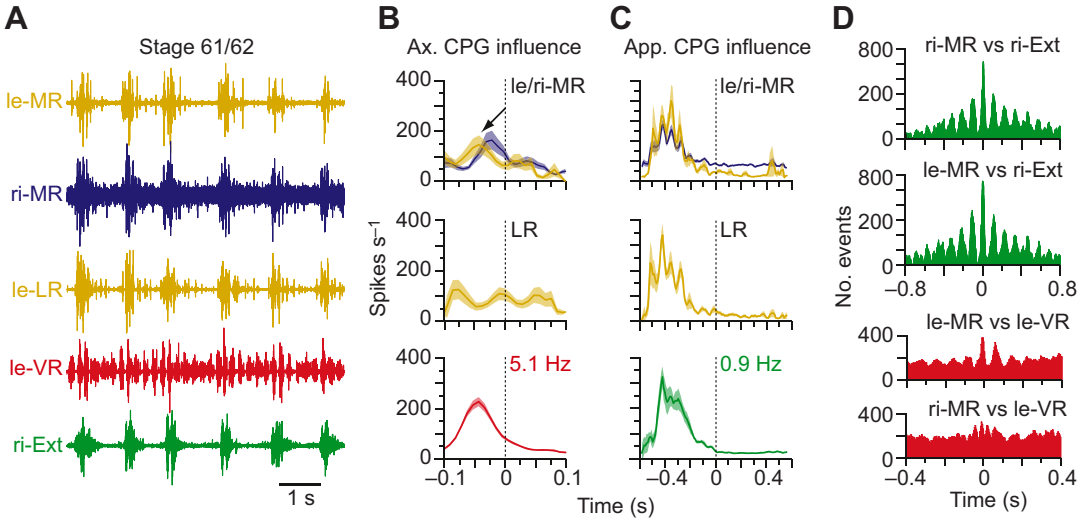

Fig. 8. Spino-extraocular motor coupling during spontaneous bimodal fictive swimming at post-climax. (A) Bilateral MR and left LR nerve activity during combined axial- and limb-based fictive swimming in a stage 61/62 preparation displaying a strong influence of Ext-timed bursting and a weak influence of the axial CPG rhythm on extraocular motor nerve activity. (B,C) Mean (±s.e.) firing rate modulation in bilateral MR and le-LR nerve over a single axial rhythm cycle (B; averaged from 22 consecutive le-VR bursts) and appendicular rhythm cycle (C; averaged from seven ri-Ext bursts). Note the small phase difference between bilateral LR nerve firing profiles (arrow in upper plot of B), but a persistence of alternating ipsilateral le-MR and le-LR discharge modulation in time with le-VR bursting. (D) Cross-correlograms confirming the strong coupling of ri-MR and le-MR nerve discharge with ri-Ext bursts (green correlograms; r^2=0.55, P<0.05 in both cases) and weaker coupling of le-MR (upper red correlogram; r^2=0.44, P=0.05) and ri-MR nerves (lower red correlogram; r^2=0.35, P=0.08) with axial le-VR motor bursts.

Journal of Experimental Biology (2016) 219, 1110-1121 doi:10.1242/jeb.136168

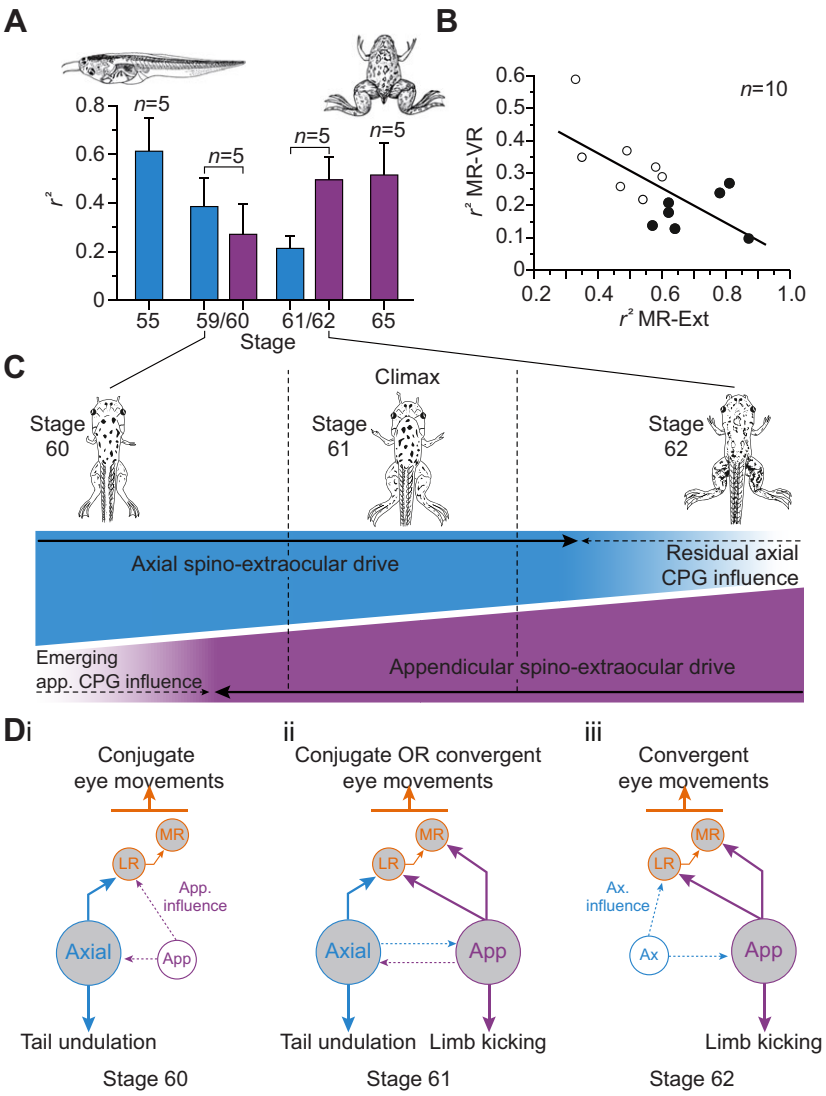

Fig. 9. Developmental plasticity in spino-extraocular motor coupling through the period of *Xenopus laevis* metamorphic climax. (A) Mean (±s.d.) correlation coefficients (r^2) indicating the strength of coupling between MR and VR (blue bars) or Ext nerve activity (purple bars) at four developmental stages. Data were obtained from five episodes in different preparations of pre-metamorphic tadpoles (stage 55), two intervening periods at metamorphic climax (stages 59/60 and 61/62) and post-metamorphic froglets (stage 65). Note the inverse relation of coupling strength between MR and axial VR activity (P<0.01; Kruskal–Wallis test) and of MR and limb Ext nerve activity (P<0.05; Kruskal–Wallis test) as metamorphosis progresses. (B) Scatter plot of correlation coefficients for MR-VR versus MR-Ext nerve activity at metamorphic climax [stages 59/60 (open circles) and 61/62 (filled circles)]. Regression analysis of pooled data from 15 episodes in 10 preparations at the two intermediate stages, shown in A, revealed a significant linear correlation (r^2=0.46, P<0.01), indicating a progressive loss of axial CPG influence and a concurrent gain of appendicular CPG control of extraocular motor activity. (C,D) Switch in predominance of axial and lumbar CPG network influence during the transition from tail- to limb-based locomotion (C) and schematic representations of functional spino-extraocular pathways (D). (Di) During coincident undulatory and appendicular swimming in early mid-metamorphic stages (59/60), efference copy signals conveyed to synergistic LR and MR extraocular motoneurons continue to arise principally from the axial CPG (ascending blue arrow), with its influence being additionally enhanced by weaker extensor-timed signals (dashed purple arrows) from the emerging hindlimb CPG (see Fig. 4). (Dii) At metamorphic climax (stage 60/61), the co-functional axial and appendicular CPGs now exert equivalent influences on the extraocular motor nuclei via independent ascending pathways (solid blue and purple arrows; see Fig. 5). (Diii) After climax (from stage 62), the influence of the primary axial CPG on extraocular motor output continues to decline (Fig. 7) until the secondary appendicular CPG becomes the sole source of spino-extraocular control at tail resorption.

are employed solely without the other. In contrast, around metamorphic climax (stages 59/60 and 61/62), when the two functional systems co-exist, the contribution of the axial CPG to spino-extraocular coupling continuously declined (blue bars in Fig. 9A), while the appendicular CPG influence gradually increased (purple bars in Fig. 9A) as one CPG emerged and replaced the other (Fig. 9A). This inversion of direct spinal CPG influence on extraocular motor control was also evident amongst animals at metamorphic climax after plotting the correlation coefficients for MR-axial VR and MR-limb nerve activity during randomly chosen fictive swim episodes in the two groups of stage 59/60 and 61/62 preparations (Fig. 9B). The linear regression of this correlation was significantly different from zero (r^2=0.46, P<0.01), indicating that an overall increase in impact of the limb CPG-extraocular motor drive (Fig. 9C, purple shading) had indeed occurred reciprocally with a parallel decline in influence of the axial CPG (Fig. 9C, blue shading).

DISCUSSION

Xenopus laevis metamorphosis from larval to adult frog is accompanied by a developmental switch from axial tail-based to limb-based locomotion. The two propulsive modes are in turn associated with the necessity to generate fundamentally different extraocular movements for offsetting self-motion-derived visual disturbances: spinal CPG efference copies produce conjugate left/right ocular movements during undulatory larval-like swimming (Lambert et al., 2012) or convergent motion of the two eyes during rectilinear adult-like kick propulsion (von Uckermann et al., 2013). Our present results show that as the appendicular motor system emerges and gradually dissociates its operation from that of the primary tail-based system (Combes et al., 2004), the spinal efference copy influence on the extraocular motor system displays a systematic variability that reflects the changing dominance of, and relationship between, the two underlying locomotor CPG networks. Thus, prior to metamorphic climax, when newly emerging limb CPG circuitry remains functionally subordinate to the primary axial CPG (Combes et al., 2004), the latter continues alone to provide the effective efference copy drive to the extraocular motor centers, as in the pre-metamorphic tadpole (Fig. 9C, left, 9Di), with the appendicular CPG at most exerting an enhancing influence on the amplitude of ongoing LR/MR motor discharge. In animals at metamorphic climax, when both locomotor systems are fully functional and can be employed concurrently, concomitant extraocular motor activity comprises a composite representation of the activity of both spinal CPGs (Fig. 9C, middle, 9Dii). Subsequently, the relative contributions of the efference copy

Journal of Experimental Biology (2016) 219, 1110-1121 doi:10.1242/jeb.136168

signals from the axial and hindlimb CPGs to extraocular motor control switch, with the latter's influence becoming increasingly dominant as metamorphosis progresses to completion (Fig. 9C, right, 9Diii).

Functionally appropriate switch of reference frames for head motion

The switch in locomotor mode at metamorphic climax necessarily leads to a change in the vectorial composition of head/body motion dynamics. While alternating horizontal angular head accelerations predominate during larval tail-based swimming, hindlimb kick propulsion in adult frogs produces mostly translational accelerations (Beyeler et al., 2008; Lambert et al., 2012; von Uckermann et al., 2013). An estimation of the spatio-temporal adequacy of the resultant eye movements during single or combined locomotor modes at metamorphic climax can be made by comparing extraocular motor responses during such self-generated motion with the characteristics of angular and linear vestibulo-ocular reflexes arising from passively imposed motion (Lambert et al., 2008). Spatio-temporally effective image stabilization during passive rotational and translational/tilt head/body movement results from sensory-motor transformations in vestibulo-ocular circuits that rely on a decomposition of 3D motion profiles into vectorial components by the different semicircular canal and otolith organs (Straka and Dieringer, 2004; Angelaki and Hess, 2005). Depending on the particular motion profile and corresponding vestibular end-organ activation, image stabilization is achieved by additive combinations of conjugate and vergent ocular movements (Straka and Dieringer, 2004): rotational or transverse linear (left–right sideward) motion elicits oppositely directed conjugate eye movements, whereas forward–backward translational oscillations trigger convergent and divergent ocular movements, respectively (Rohregger and Dieringer, 2002).

Like the combinatorial conjugate/disconjugate eye movements elicited by passive motion, our results indicate that in swimming *X. laevis* at metamorphic climax, similar extraocular motor responses are triggered by intrinsic efference copy signaling arising conjointly from the two co-functional spinal CPGs. Here, the motion vectors associated with the two locomotor modes are equivalent to passive rotational (undulatory tail-based swimming) and translational/longitudinal acceleration (limb-kick propulsion), respectively. This in turn supports the conclusion that compensatory eye movements driven by CPG feed-forward signals during bimodal locomotion in the metamorphosing frog closely match those produced by conjoint motion stimulation of the semicircular canals and utricles. Thus, the spatial reference frames employed by sensory transformations or by spinal efference copy signals coincide irrespective of the degree of combinatorial activation during either passive or active motion. Despite this potential functional equivalence, however, spinal CPG–extraocular motor coupling may play a predominant role in stabilizing gaze during locomotion because, as reported recently in larval *Xenopus*, the encoding of motion at the vestibular sensory periphery (Chagnaud et al., 2015) and also probably within central vestibular circuitry itself (Lambert et al., 2012) is considerably attenuated during swimming, thus reducing the contribution of vestibulo-ocular reflexes to compensatory eye movements.

Developmental plasticity of efference copy pathways

As established previously from specific lesions in isolated CNS preparations during fictive locomotor activity, the neural pathways that are responsible for transmitting the spinal efference copy drive to extraocular motoneurons differ distinctly before and after metamorphosis. In the pre-metamorphic tadpole, axial CPG efference signals are conveyed indirectly to MR motoneurons via diagonally ascending axonal projections that initially traverse the rostral spinal cord to access LR motoneurons and internuclear neurons in the contralateral abducens nuclei (Lambert et al., 2012). These abducens interneurons re-cross the hindbrain midline and reach synergistic MR motoneurons in the opposite oculomotor nucleus. This double midline-crossing pathway thereby produces conjugate left–right eye movements in opposition to angular head excursions during larval tail-based swimming. In contrast, in the post-metamorphic young adult when locomotion is exclusively limb-based, the efference copy signal from *de novo* lumbar CPG circuitry is conveyed to LR and MR motoneurons in the extraocular motor nuclei principally via homolaterally ascending pathways (von Uckermann et al., 2013). The latter, which are likely to arise from rostral extensions of new ipsilateral lumbo-thoracic pathways that appear concomitantly with hindlimb CPG circuitry during metamorphosis (Beyeler et al., 2008), now mediate phase-coupled contractions of both MR muscles to produce convergent eye movements during the rectilinear forward displacement in each kick cycle. Our results therefore indicate that at metamorphic climax, when the axial- and limb-based locomotor systems are co-operational, the respective neural pathways for both larval and adult modes of spino-extraocular coupling are also co-engaged. Thus, when axial swimming is expressed at this transitional stage, corresponding left–right burst alternation occurs in bilateral MR motor nerves, indicating the intervention of diagonal coupling pathways, whereas during cycles of fictive limb-kicking, ipsilateral ascending pathways ensure the co-activation of the MR nerves with synchronous left–right limb Ext bursts.

While the relative impact of these spino-extraocular motor coupling pathways changes in parallel with the overall transition from larval to adult locomotor strategy, the actual dynamics of the adaptive switch are variable and complex. For example, when both CPG networks are co-active at metamorphic climax, the efference copy drive may originate from either CPG, or both, and to varying degrees from one preparation of the 'same' visually identified developmental stage to another. Moreover, because the two CPGs continue to interact functionally as metamorphosis progresses (Rauscent et al., 2009), one network's influence on the extraocular motor centers may be exerted directly by its ascending spino-extraocular motor pathways, and/or mediated indirectly via a local influence on the other neighboring CPG and its own ascending pathways. As climax approaches and appendicular movement gradually supersedes undulatory propulsion, the effective spino-extraocular motor coupling becomes increasingly homolateral, eventually leading to MR motoneurons being driven exclusively to produce bilaterally synchronous bursts in time with hindlimb Ext motor bursts prior to tail resorption. Moreover, during this transitional phase, the two CPGs may influence the two horizontal extraocular motor populations differentially, such that the axial CPG continues to activate LR motoneurons in left/right alternation while the hindlimb CPG already drives MR motoneurons in bilateral burst synchrony. Presumably, this delay in lumbar CPG-LR influence reflects differences in timing of the developmental arrival of functional ipsilateral coupling pathways to the oculomotor (MR) and abducens (LR) motor nuclei. Concomitantly, the strength of the axial CPG's diagonal ascending drive to the extraocular motor nuclei diminishes in parallel with the decrease in horizontal angular head motion because

of the progressively weakening tail musculature, to eventually cease entirely with the tail's disappearance. Whether the primary coupling pathways present in larvae are also in the process of degeneration or reassignment to another function as in other metamorphosing neural systems (Omerza and Alley, 1992; Consoulas et al., 2000) remains to be determined. Nonetheless, despite this complexity in the developmental plasticity of internetwork connectivity during *X. laevis* metamorphosis, spinal CPG–extraocular motor influence remains constantly adapted to the spatio-temporal requirements for effective gaze stabilization, regardless of whether the locomotor strategy is axial or appendicular (or both), and through a period when the dynamic equilibrium between the two propulsive modes themselves is progressively changing.

Neural network interactions and development

The developmental evolution in locomotor–extraocular motor coupling during frog metamorphosis is also conceptually instructive in comparison with other interacting motor systems. Coordinating central nervous interactions between functionally distinct and otherwise independent motor networks include those responsible for locomotion and respiratory activity in a variety of animals (Bramble and Carrier, 1983; Funk et al., 1992; Morin and Viala, 2002; Gariépy et al., 2012), avian breathing and vocalization (Manogue and Paton, 1982), and pyloric and gastric motor output of the crustacean stomatogastric system (Bartos and Nusbaum, 1997; Clemens et al., 1998). However, an important difference between these examples and *X. laevis* locomotor–extraocular motor coupling is that they involve networks that are each intrinsically capable of independent rhythmogenic operation. Thus their coordination can range from a momentary or harmonic alteration of one rhythm by the other, to complete synchronization. Here, when the rhythmogenic spinal network for self-motion is active, the inherently non-rhythmic extraocular system becomes entirely appropriated to cyclic feed-forward copies of locomotor CPG output, similar to recently described tentacle movements in *X. laevis* tadpoles during swimming, when spinal CPG efference copies drive bilateral trigeminal motoneurons (Hänzi et al., 2015). However, when locomotion ceases and CPG circuitry falls inactive, the extraocular motor system now becomes completely subservient to extrinsic feedback signaling from the visuo-vestibular sensory systems during any passively induced head/body motion (Straka and Dieringer, 2004; Cullen, 2012).

Xenopus laevis spinal CPG–extraocular motor coupling further differs fundamentally from other interacting motor systems in that it undergoes a secondary phase of development during which the fates of the constituent networks are completely different: on the one hand, a primary locomotor system that disappears and is supplanted by an entirely different one (Combes et al., 2004); on the other hand, an extraocular motor system, including its neuromuscular machinery and central control circuitry, that has already been established during post-embryonic larval life and remains essentially unchanged through metamorphosis and into adulthood (Straka and Dieringer, 2004; Lambert et al., 2008). Indeed it is this differential developmental timetable that, for effective gaze stabilization to be ensured throughout the metamorphic period, requires both a rewiring of the pathways by which the two motor systems intercommunicate and a gradual switching in pathway allegiance as one locomotory system supersedes the other. More generally, the change in CPG efference copy signaling and spino-extraocular motor coupling associated with the metamorphic locomotor development of *X. laevis* is a striking example of the extent to which the vertebrate nervous system can undergo adaptive modifications in order to constantly sustain adequate functionality.

Acknowledgements

The authors are grateful to Gilles Courtand (INCIA) for technical support with image processing.

Competing interests

The authors declare no competing or financial interests.

Author contributions

G.v.U., F.M.L., D.C., H.S. and J.S. planned the experiments, G.v.U., F.M.L. and D.C. acquired and analyzed the data, and G.v.U., F.M.L., D.C., H.S. and J.S. wrote the manuscript.

Funding

This work was funded by the French 'Agence Nationale de la Recherche' (ANR-08-BLAN-0145-01, 'Galodude'; ANR-15-CE32-0007-01, 'Locogaze'), the German Science Foundation (CRC 870, B12) and the German Federal Ministry of Education and Research (01 EO 0901). We are also grateful for financial support from the Bayerisch-Französisches Hochschulzentrum (BFHZ).

References

Angelaki, D. E. and Cullen, K. E. (2008). Vestibular system: the many facets of a multimodal sense. *Annu. Rev. Neurosci.* **31**, 125-150.
Angelaki, D. E. and Hess, B. J. M. (2005). Self-motion-induced eye movements: effects on visual acuity and navigation. *Nat. Rev. Neurosci.* **6**, 966-976.
Azizi, E., Landberg, T. and Wassersug, R. J. (2007). Vertebral function during tadpole locomotion. *Zoology* **110**, 290-297.
Bartos, M. and Nusbaum, M. P. (1997). Intercircuit control of motor pattern modulation by presynaptic inhibition. *J. Neurosci.* **17**, 2247-2256.
Beyeler, A., Métais, C., Combes, D., Simmers, J. and Le Ray, D. (2008). Metamorphosis-induced changes in the coupling of spinal thoraco-lumbar motor outputs during swimming in *Xenopus laevis*. *J. Neurophysiol.* **100**, 1372-1383.
Bramble, D. M. and Carrier, D. R. (1983). Running and breathing in mammals. *Science* **219**, 251-256.
Chagnaud, B. P., Simmers, J. and Straka, H. (2012). Predictability of visual perturbation during locomotion: implications for corrective efference copy signaling. *Biol. Cybern.* **106**, 669-679.
Chagnaud, B. P., Banchi, R., Simmers, J. and Straka, H. (2015). Spinal corollary discharge modulates motion sensing during vertebrate locomotion. *Nat. Comm.* **6**, 7982.
Clemens, S., Combes, D., Meyrand, P. and Simmers, J. (1998). Long-term expression of two interacting motor pattern-generating networks in the stomatogastric system of freely behaving lobster. *J. Neurophysiol.* **79**, 1396-1408.
Combes, D., Merrywest, S. D., Simmers, J. and Sillar, K. T. (2004). Developmental segregation of spinal networks driving axial- and hindlimb-based locomotion in metamorphosing *Xenopus laevis*. *J. Physiol.* **559**, 17-24.
Combes, D., Le Ray, D., Lambert, F. M., Simmers, J. and Straka, H. (2008). An intrinsic feed-forward mechanism for vertebrate gaze stabilization. *Curr. Biol.* **18**, R241-R243.
Consoulas, C., Duch, C., Bayline, R. J. and Levine, R. B. (2000). Behavioral transformations during metamorphosis: remodeling of neural and motor systems. *Brain Res. Bull.* **53**, 571-583.
Cullen, K. E. (2004). Sensory signals during active versus passive movement. *Curr. Opin. Neurobiol.* **14**, 698-706.
Cullen, K. E. (2011). The neural encoding of self-motion. *Curr. Opin. Neurobiol.* **21**, 587-595.
Cullen, K. E. (2012). The vestibular system: multimodal integration and encoding of self-motion for motor control. *Trends Neurosci.* **35**, 185-196.
Finch, D. J. and Collett, T. S. (1983). Small-field, binocular neurons in the superficial layers of the frog optic tectum. *Proc. R. Soc. Lond. B Biol. Sci.* **217**, 491-497.
Funk, G. D., Steeves, J. D. and Milsom, W. K. (1992). Coordination of wingbeat and respiration in birds. II. "Fictive" flight. *J. Appl. Physiol.* **73**, 1025-1033.
Gariépy, J.-F., Missaghi, K., Chevallier, S., Chartré, S., Robert, M., Auclair, F., Lund, J. P. and Dubuc, R. (2012). Specific neural substrate linking respiration to locomotion. *Proc. Natl. Acad. Sci. USA* **109**, E84-E92.
Hänzi, S., Banchi, R., Straka, H. and Chagnaud, B. P. (2015). Locomotor corollary activation of trigeminal motoneurons: coupling of discrete motor behaviors. *J. Exp. Biol.* **218**, 1748-1758.
Hoff, K. v. S. and Wassersug, R. J. (1986). The kinematics of swimming in larvae of the clawed frog, *Xenopus laevis*. *J. Exp. Biol.* **122**, 1-12.
Lambert, F. M., Beck, J. C., Baker, R. and Straka, H. (2008). Semicircular canal size determines the developmental onset of angular vestibuloocular reflexes in larval *Xenopus*. *J. Neurosci.* **28**, 8086-8095.

Lambert, F. M., Combes, D., Simmers, J. and Straka, H. (2012). Gaze stabilization by efference copy signaling without sensory feedback during vertebrate locomotion. *Curr. Biol.* **22**, 1649-1658.
Manogue, K. R. and Paton, J. A. (1982). Respiratory gating of activity in the avian vocal control system. *Brain Res.* **247**, 383-387.
Morin, D. and Viala, D. (2002). Coordinations of locomotor and respiratory rhythms in vitro are critically dependent on hindlimb sensory inputs. *J. Neurosci.* **22**, 4756-4765.
Nieuwkoop, P. D. and Faber, J. (1956). *Normal Table of Xenopus laevis (Daudin). A Systematical and Chronological Survey of the Development from the Fertilized Egg Till the End of Metamorphosis*. Amsterdam: North Holland.
Omerza, F. F. and Alley, K. E. (1992). Redeployment of trigeminal motor axons during metamorphosis. *J. Comp. Neurol.* **325**, 124-134.
Rauscent, A., Einum, J., Le Ray, D., Simmers, J. and Combes, D. (2009). Opposing aminergic modulation of distinct spinal locomotor circuits and their functional coupling during amphibian metamorphosis. *J. Neurosci.* **29**, 1163-1174.
Rohregger, M. and Dieringer, N. (2002). Principles of linear and angular vestibuloocular reflex organization in the frog. *J. Neurophysiol.* **87**, 385-398.
Straka, H. and Dieringer, N. (2004). Basic organization principles of the VOR: lessons from frogs. *Prog. Neurobiol.* **73**, 259-309.
Straka, H. and Simmers, J. (2012). *Xenopus laevis*: an ideal experimental model for studying the developmental dynamics of neural network assembly and sensory-motor computations. *Dev. Neurobiol.* **72**, 649-663.
von Uckermann, G., Le Ray, D., Combes, D., Straka, H. and Simmers, J. (2013). Spinal efference copy signaling and gaze stabilization during locomotion in juvenile *Xenopus* frogs. *J. Neurosci.* **33**, 4253-4264.